Supplement of The Cryosphere, 10, 1427–1432, 2016
http://www.the-cryosphere.net/10/1427/2016/
doi:10.5194/tc-10-1427-2016-supplement

The Cryosphere
Open Access

Supplement of

Brief Communication: Twelve-year cyclic surging episodes at Donjek Glacier in Yukon, Canada

Takahiro Abe et al.

Correspondence to: Takahiro Abe (abetaka@frontier.hokudai.ac.jp)

Supplementary material of “Twelve-year cyclic surging episode at Donjek Glacier in Yukon, Canada” by Abe et al.

This supplementary material documents the data list and the detailed processing method. After that, we show the spatial patterns in ice velocity and the terminus area change at Donjek Glacier.

1. Methodology

We selected 66 pairs of the Landsat images (Table S1) and applied the CCF-O method to the band 4 images (30 m resolution) for Landsat 4 and 5 and the band 8 images (15 m resolution) for Landsat 7 and 8. After co-registration of the two images, we computed the cross-correlation coefficients with a reference chip (30 × 30 pixels) and a search chip (50 × 50 pixels) on the orientation images. The step number was set as 6 × 6 pixels. The distance between the maximum peaks of the two images was regarded as a displacement of glacier.

After performing the CCF-O, the median filters about magnitude and flow direction were performed in each result within areas of 3 × 3 or 5 × 5 pixels to reject the outliers and to smooth the results. The velocity errors of ice speed ranged between 0.09 and 0.80 m/d, which wass estimated by the mean speed of non-glacier area clipped by the Randolph Glacier Inventory version 4.0 glacial masks (Pfeffer et al., 2014). The error was dependent on the time separations between the image acquisitions, which were less than about 4 months. Thus, some pairs could include the seasonal speed-up, but the amplitude was much smaller than that in the surging episodes. We also confirmed that the orientations of the displacement vectors were identical to the flow direction of the glacier. However, it was harder to track the surface features in the accumulation area due to its low contrast. Thus, our velocity data indicate the poorer coverage in the upstream region. We averaged the velocity data over the 450 × 450-m^2 area and every 300 m intervals along the flow line set from the terminus (Fig. 1a).

We also examined the terminus area changes associated with the surging events using the composite false images of bands 4–6 for the Landsat 1–3 MSS, 2–4 for the Landsat 4/5 MSS, 3–5 for the Landsat 5 TM and the Landsat 7 ETM+, and 4–6 for the Landsat 8 OLI. These band combinations take advantage of the clear contrast between ice and rock (McNabb and Hock, 2014).

2. Spatial patterns in ice velocity

Figure S1 shows some snapshots of spatial patterns in ice velocity at Donjek Glacier. The speed patterns associated with three surging episodes in 1989, 2001, and 2013 are shown in Figs. 2b, d, and f. The measured maximum speed is about 2 m/d, 4.5 m/d, and 3 m/d, respectively. The others are in its quiescent phase, whose speeds are about 0.5 m/d or below. The higher velocity area is limited to the ~20 km section from the terminus (Figs. 2a, b, and e), which indicates it is associated with the geometry mentioned in the main text.

3. Terminus area change

Figure S2 shows the spatial and temporal changes in the terminus area from 1973 to 2014 on the Landsat 8 OLI band 8 image. The color line shows the terminus position in each image. The gradual decrease of the terminus area is shown in this figure.

4. Surface slope angle

Figure S3 shows the slope angles along the flow line used in Fig. 1c derived from two Aster DEMs (blue in 28 September 2001, and red in 26 May 2002) and Aster GDEM (green). The Black line shows the width of the valley. Although GDEM is composite DEM and we don't know the exact date, all the three curves indicate peaks around 18.5 and 22 km point. The former point corresponds the initiation point of S-shape valley, and the latter is that of narrowing valley. These indicate that the valley constriction could generate the slope steepening. Moreover, comparing the blue and red curve especially in the section between 18 and 19.5 km, the slope in 2002 (red) is clearly larger than that in 2001 (blue). This is consistent with our suggestion that the ice had been thickened after the peak speed in the 2001 episode.

5. References

McNabb, R. W., and Hock, R.: Alaska tidewater glacier terminus positions, 1948–2012, J. Geophys. Res. Earth Surf., 119, 153–167 , 2014.

Pfeffer, W. T., Arendt, A. A., Bliss, A., Bolch, T., Cogley, J. G., Gardner, A. S., Hagen, J.-O., Hock, R., Kaser, G., Kienholz, C., Miles, E. S., Moholdt, G., Mölg, N., Paul, F., Radić, V., Rastner, P., Raup, B. H., Rich, J., Sharp, M. J. and the Randolph consortium: The Randolph Glacier Inventory: a globally complete inventory of glaciers, J. Glaciol., 60, 537–552, 2014.

Table S1. The detail of the image pairs to derive the velocity field.

Satellite/Sensor	Image1	Image2	Span (day)	Satellite/Sensor	Image1	Image2	Span (day)
Landsat4-5/TM+	19860716	19860911	57	Landsat7/ETM+	20080424	20080526	32
	19870728	19870829	32		20080526	20080627	32
	19880628	19880806	39		20080627	20080830	64
	19890608	19890827	80		20080830	20081001	32
	19900625	19900812	48		20090427	20090716	80
	19910723	19910925	64		20090716	20090801	16
	19930525	19930728	64		20090801	20090902	32
	19930728	19930813	16		20090902	20090918	16
	19940426	19940715	80		20090918	20091020	32
	19940715	19940816	32		20100601	20100804	64
	19950429	19950515	16		20100804	20100921	48
	19970520	19970815	87		20120419	20120606	48
	19970815	19970925	41		20120606	20120708	32
	19980701	19980928	89		20120816	20120917	32
	20110806	20111002	57		20130321	20130406	16
Landsat7/ETM+	19990705	19990829	55	Landsat8/OLI	20130414	20130516	32
	20000504	20000707	64		20130523	20130624	32
	20000730	20001002	64		20130624	20130811	48

20010327	20010428	32	20130811	20130827	16
20010421	20010523	32	20130905	20131108	64
20010523	20010608	16	20131108	20140203	87
20010608	20010624	16	20140203	20140219	16
20010701	20010802	32	20140219	20140323	32
20010802	20010903	32	20140401	20140503	32
20020307	20020408	32	20140503	20140604	32
20020408	20020526	48	20140526	20140611	16
20020526	20020805	71	20140604	20140722	48
20030411	20030427	16	20140722	20140807	16
20030427	20030716	80	20140807	20140823	16
20030716	20030817	32	20140823	20140908	16
20030817	20031020	64	20140908	20140924	16
20040413	20040803	112	20141001	20141017	16
20060505	20060910	128	20141017	20141127	41
20070609	20070828	80			

Figures and captions

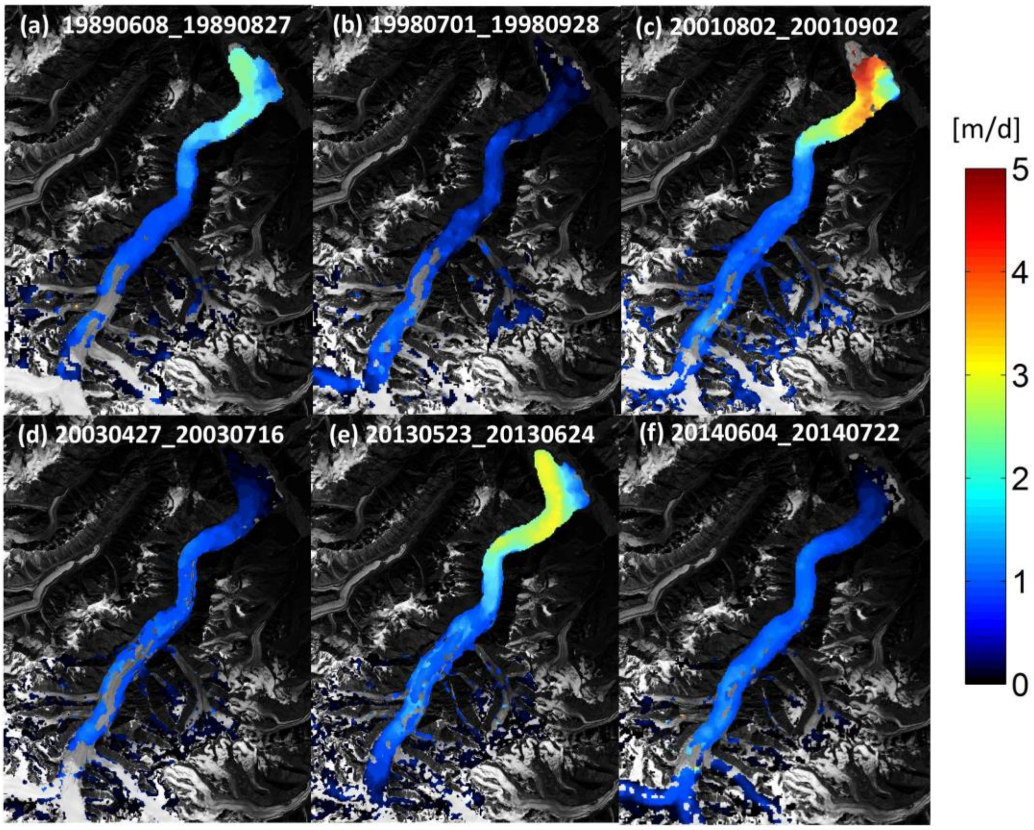

Figure S1. Some examples of spatial patterns in the ice speed. The color scale is shown in linear scale.

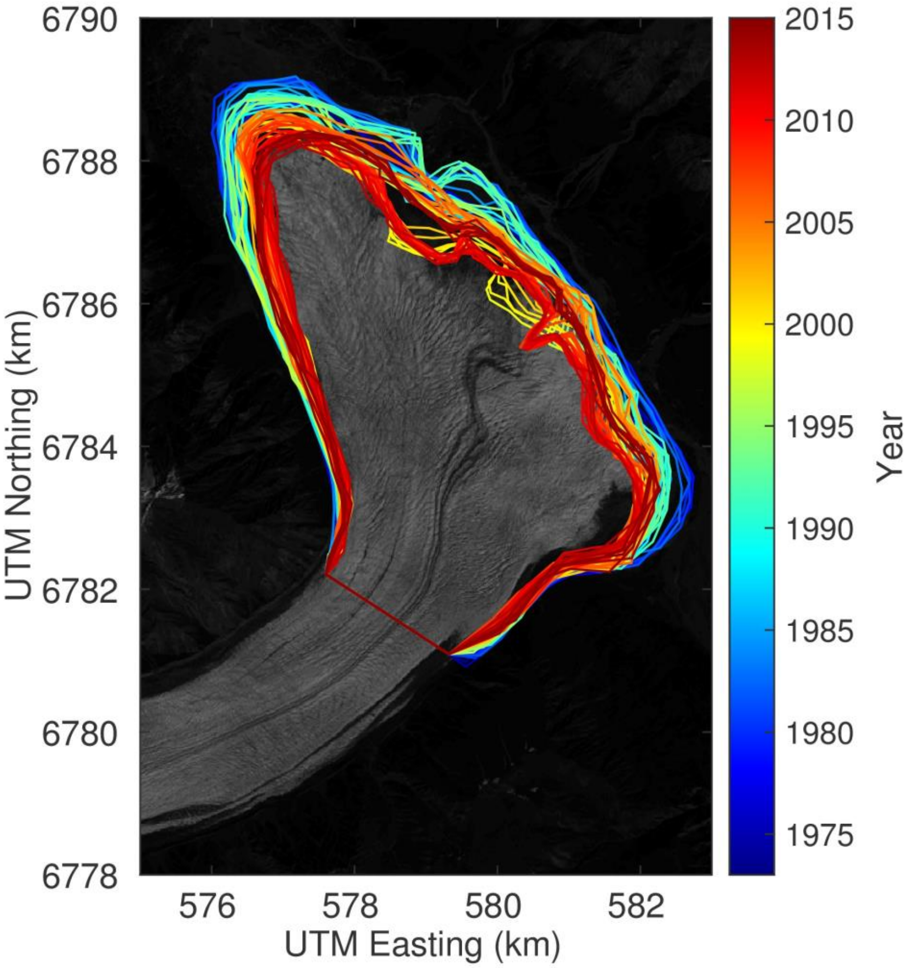

Figure S2. Spatial and temporal changes in the terminus area from 1973 to 2014.

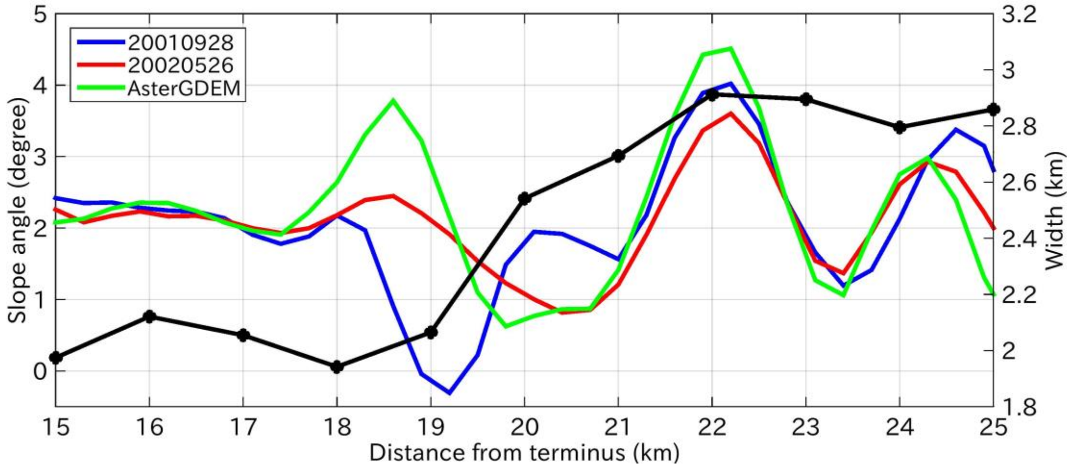

Figure S3. Slope angles along the flow line used in Fig. 1c. The blue and red line show the slope angle derived from two Aster DEMs on 28 September 2001, and 26 May 2002, respectively. The green line shows the angle derived from Aster GDEM. The black line shows the width of the valley.